

# Numerical Simulation of the Optical Properties of SiC/SiO<sub>2</sub> Quantum Dots

J. S. de Sousa, V. N. Freire, G. A. Farias,

*Departamento de Física, Universidade Federal do Ceará,  
Campus do Pici, Caixa Postal 6030, 60455-900 Fortaleza, Ceará, Brazil*

and E. F. da Silva Jr.

*Departamento de Física, Universidade Federal de Pernambuco,  
Cidade Universitária, 50670-901 Recife, Pernambuco, Brazil*

Received on 27 March, 2003

We perform a theoretical investigation of the absorption and emission properties of quantum confined SiC/SiO<sub>2</sub> spherical quantum dots, focusing on the size-dependent emission and absorption spectra of an independent single dot. We observed strong oscillations in the absorption lines as a consequence of the interband transitions rules, and a blue-shift of the emission spectra lines with the decrease of the quantum dot diameter.

## 1 Introduction

Despite of the considerable achievements in the SiC growth technology over the recent years, several problems concerning the basic physical properties still stand. The electronic structure of SiC has been calculated by several mathematical methods including Orthogonalized Plane Wave [1], Empirical Pseudopotential [2], Density Functional Theory within the Local Density Approximation [3], among others. All these techniques predicts a high anisotropic nature of the band structure leading to a tensorial effective mass, which has been confirmed by cyclotron resonance measurements [4], and the consequences of this anisotropy on the overall electrical behavior of SiC is, up to now, far from being entirely understood. However, it was recently shown that the conduction band anisotropy plays an interesting role on the energy spectra of Si/SiO<sub>2</sub> nanocrystals, which consequently may affect the electrical and optical properties of devices [5]. In another recent work, the feasibility of green-to-blue light emission was explored with the calculation of the quantum confined exciton in SiC/SiO<sub>2</sub> quantum wires [6]. Depending on the confinement dimension and interface width, different SiC polytypes may be used specifically for applications in different spectral regions from green to ultraviolet emissions: the 3C-SiC polytype seems to be the best choice for green light emission, while 6H-SiC and 4H-SiC are more suitable for blue and blue-ultraviolet light emission, respectively.

In this paper, we aim into a better understanding of the optical absorption and emission spectra of SiC/SiO<sub>2</sub> quantum dots (QD's) by taking account of the tensorial nature of the effective mass of the system. Within the authors knowledge, SiC/SiO<sub>2</sub> quantum dots were still not synthe-

sized to date, and therefore we aim also to anticipate and stimulate experimental work, on optical characteristics of the SiC/SiO<sub>2</sub> system with respect to quantum dot size and the anisotropy of the SiC/SiO<sub>2</sub> system.

## II - Numerical Model

Figure 1 exhibits the simulation unit cell used in this work. We focus on a single QD by assuming that adjacent QD's are positioned far enough from each other in such way that the penetration of the wavefunctions into the oxide layer becomes negligible before overlapping with other lateral nanocrystal wavefunctions.

The Schrodinger equation is discretized using a finite-difference scheme in a tridimensional rectangular grid leading to a sparse seven banded matrix, from which we extract the energy states and wavefunctions. The effective mass approximation is used by taking into account the complicated anisotropic features of the SiC polytypes, in such way that the effective mass is no longer a number, but a tensor of first rank. Within this context, the Schrodinger equation to be solved has the following form:

$$[\hat{\nabla}^T \hat{\sigma} M(\mathbf{r})^{-1} \hat{\sigma}^{-1} \hat{\nabla} + \Delta E_C(\mathbf{r})] \Psi_i(\mathbf{r}) = E_i \Psi_i(\mathbf{r}) \quad (1)$$

where  $M(\mathbf{r})^{-1}$  is the 3x3 diagonal inverse effective mass tensor whose diagonal is given by  $m_1(\mathbf{r})^{-1}$ ,  $m_2(\mathbf{r})^{-1}$ ,  $m_3(\mathbf{r})^{-1}$ . These quantities represent the effective masses values related to the main ellipsoidal radius of the valleys of

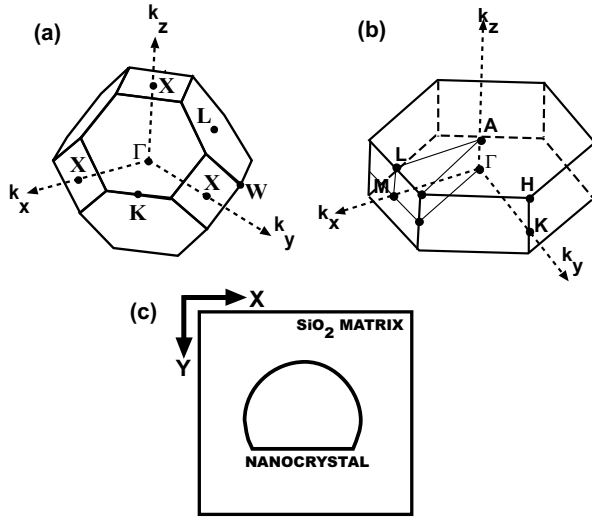


Figure 1. Schematics of the Brillouin zones for the 3C- (a) and 4H- (b) SiC polytypes and the main symmetry points of both zones. It is also plotted the simulation unit cell containing a single QD (c).

energy minima.  $\nabla$  is the momentum operator represented by a column vector. The transformation matrix  $\hat{\sigma}$  describes the rotation of the SiC crystallographic directions with respect to the dot axes. The quantity  $\Delta E_C(\mathbf{r})$  accounts for the band gap discontinuity. Details on the computational model are given elsewhere [7].

The key parameters of the model discussed above are the directional effective masses of the ellipsoid of energy and their directions in the Brillouin zone. However, due to the variety of polytypes, SiC can be grown in three different crystalline structures: cubic(zincblend), hexagonal(wurtzite) and rhombohedral. 4H-SiC is 100% hexagonal, 3C-SiC is 100% cubic, and the other types have a different degree of hexagonality. The band structure is highly anisotropic for all polytypes, and SiC has an indirect band gap with the minima of the conduction band localized in different points of the reciprocal space, depending on the crystalline structure of the polytype. For example, 4H-SiC has a minimum of energy at the highly symmetric point  $M$  with the main axes of the energetic ellipsoid pointing to  $M\Gamma$  ( $m_1$ ),  $MK$  ( $m_2$ ) and  $ML$  ( $m_3$ ). Therefore, Schrodinger equation needs to be solved 6 times, one for each point  $M$  of the hexagonal Brillouin zone. Moreover, the ellipsoids of energy are rotated around the  $k_z$  axis by increments  $60^\circ$  with respect to each other, and a different rotation operator  $\hat{\sigma}$  in Eq. 1 needs to be assigned for each energy valley to match appropriate alignment with simulation cell axes (see Figure 1).

The calculations of the optical properties of the SiC QD's is based on the Fermi's golden rule, where the absorption and emission spectra are proportional to the quantity:

$$R_T^{u,l}(\omega) = n_l n_u' W_{AB}^{u,l}(\omega) - n_l' n_u W_{EM}^{u,l}(\omega) \quad (2)$$

The equation above yields the net transition rate between a lower  $l$  and an upper  $u$  confined states, and must be summed over all six conduction band valleys, light and heavy holes bands, and subbands indexes. The quantities  $n_{u,l}$  and  $n_{u,l}'$  indicates the occupation and de-occupation of the upper and

lower states, respectively. For higher temperatures, Fermi-Dirac statistics should be used. However, due to the low dimensionality of the structure, the energy levels inside the QD's are reasonably well separated such that thermal fluctuation of the electron occupation at room temperature are negligible and the single electron charging model is still valid (Coulomb blockade regime). Details of this model are given in reference [5]. Therefore,  $n_{u,l}$  and  $n_{u,l}'$  assume the integer values 0,1 and 2, since individual spins are neglected. For the sake of simplicity, we also disregard the many body interactions among the carriers.  $W_{AB}^{u,l}(\omega)$  and  $W_{EM}^{u,l}(\omega)$  represent the photon absorption and emission probabilities per unit second due to the incident light with frequency  $\omega$ , respectively. The formalism used here is discussed in reference [8].

## 2 Results

Figure 2 depicts the absorption (top) and band gap luminescence (bottom) spectra for an spherical 4H-SiC/SiO<sub>2</sub> QD. Our calculations focus on the optical properties of a single QD. This fact can be observed in the absorption lines, which exhibits an strong oscillatory behavior. These oscillations are consequence of the interband transitions rules. In typical experimental absorption spectra, these oscillations are not observed because of the broadening of the absorption lines caused by the size distribution of the QD's in the sample. The same broadening is commonly observed in the experimental luminescence spectra. In order so simulate such experimental broadening, it is necessary to calculate a large number of confined states for an ensemble of quantum dots with a size distribution. This is computationally intense, and we reserve this topic for future study.

In Fig. 2, it is observed a strong variation on the width of the absorption lines for different QD diameters. The figure shows that 5 nm wide QD's absorb light in a range of 1.1 eV while the 9 nm absorbs in a spectral range of approximately 0.4 eV. This is a consequence of the limited number of calculated confined states. In this paper, we considered the total of 20 states for each band, with valence band entirely filled, and the conduction empty. The energy range covered by these 20 states in the 5 nm wide QD is larger than in the 9 nm case. In the case of the luminescence spectra, we only investigated the bandgap emission, where the assumption that electrons excited to higher states in conduction band thermalize down to the ground state before recombining with holes in the valence band. In both cases, one can observe the expected blue-shift of the spectral lines with a decrease of the QD size.

## 3 Concluding Remarks

In conclusion, we addressed the characteristics of the optical absorption and emission spectra of SiC/SiO<sub>2</sub> quantum dots (QD's) by taking into account the tensorial nature of the effective mass and focusing on a single QD. Our results exhibits strong oscillations in the absorption line as a consequence of the transitions rules between the conduction and

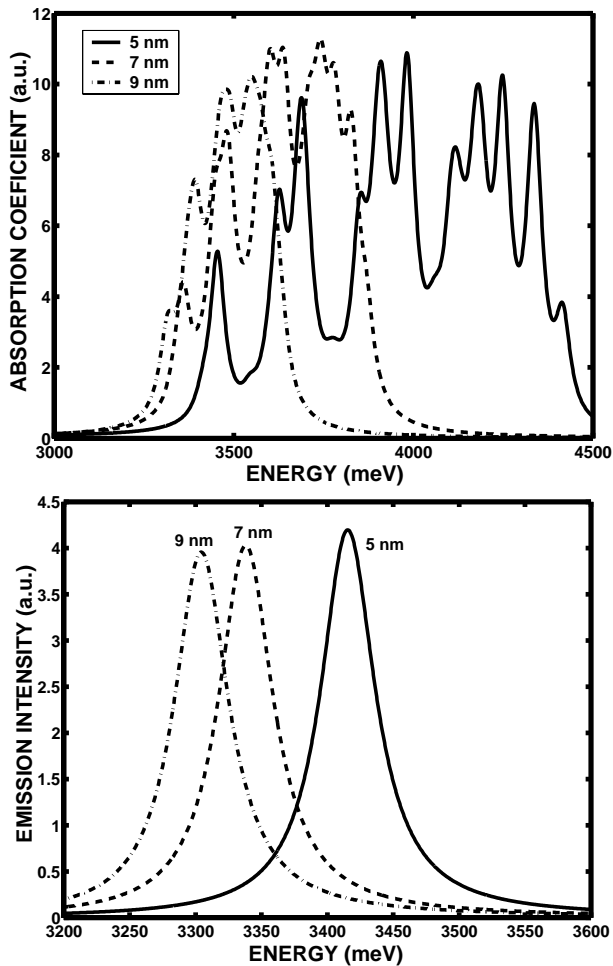


Figure 2. Absorption(top) and emission(bottom) spectra for a spherical 4H-SiC QD with 5,7 and 9 nm of diameter.

valence bands, and a blue-shift of the spectral lines with a decrease of the QD size is observed. Since SiC QD's were

not grown yet, these results must be faced as a preliminary study and we hope to stimulate experimental observations on this matter.

### Acknowledgements

The authors would like to acknowledge the financial support received from the Science Funding Agency of the Ceará (FUNCAP), the Brazilian National Research Council (CNPq) through grant # 550.015/01-09/NanoSemiMat, and the Ministry of Planning (FINEP) through CTPETRO under contract # 65.00.02.80.00.

### References

- [1] F. Herman, J. P. Van Dyke and R. L. Kortum, *Mat. Res. Bull.* **4**, 5167 (1969).
- [2] L. A. Hamstreet and C. Y. Fong, in *Silicon Carbide-1973*, edited by R. C. Marshall, J. W. Faust and C. E. Ryan (Univ. of South Carolina Press, Columbia, South Carolina 1974), pp. 284.
- [3] W. R. L. Lambrecht, S. Limpijumnong, S. N. Rashkeev and B. Seagall, *Phys. Stat. Sol. B* **202**, 5 (1997).
- [4] W. R. L. Lambrecht and B. Seagall, *Phys. Rev. B* **52**, 2249 (1995).
- [5] A. Thean, J. P. Leburton, *J. Appl. Phys.* **89**, 2808 (2001).
- [6] J. S. de Sousa, H. Wang, V. N. Freire, G. A. Farias and E. F. da Silva Jr., *Journal of the Korean Physical Society* **39**, 443 (2001).
- [7] J. S. de Sousa, A. V. Thean, J.-P. Leburton and V. N. Freire, *J. Appl. Phys.* **92**, 6182 (2002).
- [8] S. L. Chuang, in *Physics of Optoelectronic Devices*, Wiley Series in Pure and Applied Optics (1995), ch. 9.